nature cell biology

Whacked and Rab35 polarize dynein-motor-complex-dependent seamless tube growth

Jodi Schottenfeld-Roames[1] and Amin S. Ghabrial[1,2]

Seamless tubes form intracellularly without cell–cell or autocellular junctions. Such tubes have been described across phyla, but remain mysterious despite their simple architecture. In *Drosophila*, seamless tubes are found within tracheal terminal cells, which have dozens of branched protrusions extending hundreds of micrometres. We find that mutations in multiple components of the dynein motor complex block seamless tube growth, raising the possibility that the lumenal membrane forms through minus-end-directed transport of apical membrane components along microtubules. Growth of seamless tubes is polarized along the proximodistal axis by Rab35 and its apical membrane-localized GAP, Whacked. Strikingly, loss of *whacked* (or constitutive activation of Rab35) leads to tube overgrowth at terminal cell branch tips, whereas overexpression of Whacked (or dominant-negative Rab35) causes formation of ectopic tubes surrounding the terminal cell nucleus. Thus, vesicle trafficking has key roles in making and shaping seamless tubes.

Three tube types—multicellular, autocellular and seamless—are found in the *Drosophila* trachea[1,2]. Most tracheal cells contribute to multicellular tubes or make themselves into unicellular tubes by wrapping around a lumenal space and forming autocellular adherens junctions, but two specialized tracheal cell types, fusion cells and terminal cells, make 'seamless' tubes[1,3,4]. How seamless tubes are made and how they are shaped are largely unknown. One hypothesis holds that seamless tubes are built by 'cell hollowing'[5,6], in which vesicles traffic to the centre of the cell and fuse to form an internal tube of apical membrane, whereas an alternative model proposes that apical membrane is extended internally from the site of intercellular adhesion[7]. In both models, transport of apical membrane would probably play a key role. As terminal cells make seamless tubes continuously during larval life, they serve as an especially sensitive model system in which to dissect the genetic program.

Tracheal cells are initially organized into epithelial sacs with their apical surface facing the sac lumen. During tubulogenesis, γ-tubulin becomes localized to the lumenal membrane of each tracheal cell, generating microtubule networks oriented with minus ends towards the apical membrane[8]. Terminal and fusion cells are first selected as tip cells[1] that undergo a partial epithelial-to-mesenchymal transition and initiate branching morphogenesis: they lose all but one or two cell–cell contacts and become migratory[9,10]. Branchless-FGF signalling induces a subpopulation of tip cells to differentiate as terminal cells[9]. During larval life, terminal cells ramify on tissues spread across several hundred micrometres, with branching patterns that reflect local hypoxia[11]. A single seamless tube forms within each branched extension of the terminal cell.

How trafficking contributes to seamless tube morphogenesis is unknown. Despite clues that vesicle transport plays a role in the genesis of seamless tubes, the tube morphogenesis genes remain elusive[7,11–13]. Here we characterize the cytoskeletal polarity of larval terminal cells, show that a minus-end-directed microtubule motor complex is required for seamless tube growth and characterize mutations in *whacked* (*wkd*) that uncouple seamless tube growth from the normal spatial cues. Sequence analysis indicates that *wkd* encodes a RabGAP, and we show that Rab35 is the essential target of Wkd, and that together, Wkd and Rab35 can polarize the growth of seamless tubes.

We examined apical–basal polarity and cytoskeletal organization in mature larval terminal cells. The lumenal membrane (Supplementary Fig. S1a,b and Methods) was decorated by puncta of Crumbs, a definitive apical membrane marker[14,15] (Fig. 1a,a′,b,b′). We found actin filaments enriched in three distinct subcellular domains: surrounding seamless tubes, decorating filopodia and outlining short stretches of basolateral membrane (Fig. 1c–c″,d–d″). The microtubule cytoskeleton also seemed polarized, with γ-tubulin lining the seamless tubes and enriched at tube tips (Fig. 2a–a″,b–b″). These data are consistent with tracheal studies in the embryo[7]. EB1::GFP analyses of growing (plus-end) microtubules demonstrated that some are oriented towards the soma and others towards branch tips (Supplementary Movie S1). Stable acetylated microtubules ran parallel to the tubes (Fig. 2d–d″) and extended beyond the lumen at branch tips (Fig. 2c–c″, arrowhead)

[1]Department of Cell & Developmental Biology, University of Pennsylvania School of Medicine, 421 Curie Boulevard, 1214 BRB II/III, Philadelphia, Pennsylvania 19104, USA.
[2]Correspondence should be addressed to A.S.G. (e-mail: ghabrial@mail.med.upenn.edu)

Received 6 July 2011; accepted 3 February 2012; published online 11 March 2012; DOI: 10.1038/ncb2454

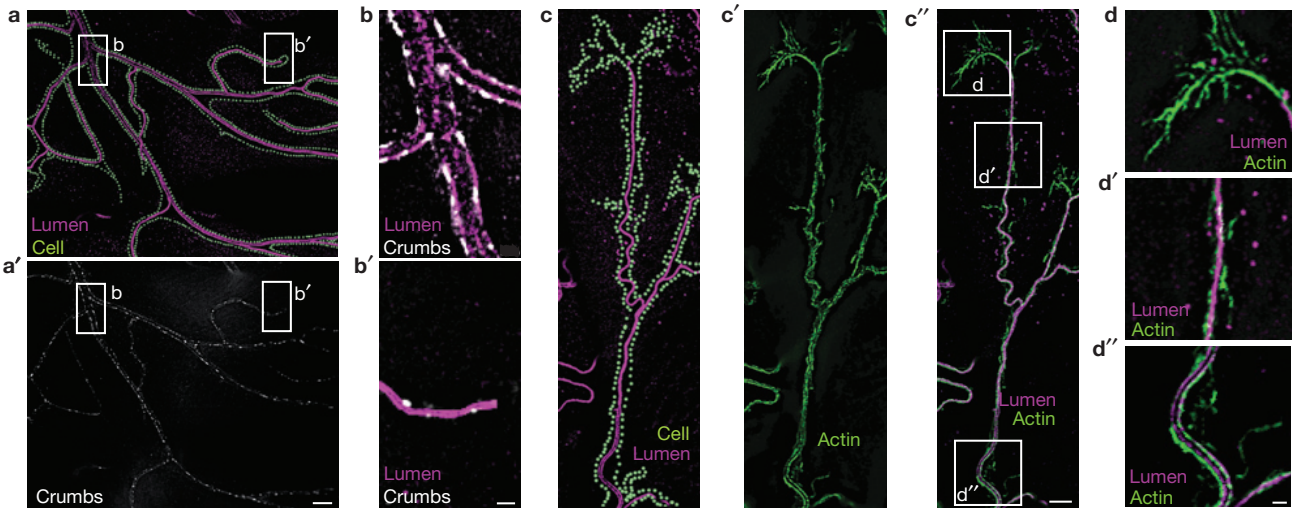

Figure 1 The lumenal membrane of tracheal terminal cells has apical identity. (**a**) A portion of a wild-type terminal cell is shown, with the cell shape outlined by dots (light green)—the cell outline layer was made by tracing actin::RFP staining with the gain increased sufficiently to visualize basolateral actin. The terminal cell is stained with α-Wkdpep sera, revealing the lumenal membrane (magenta) of seamless tubes. (**a′**) Staining (white) against a functional Crumbs::GFP fusion protein knocked into the endogenous *crumbs* locus demonstrates that the lumenal membrane of terminal cell seamless tubes is apical. (**b**,**b′**) White rectangles in **a**,**a′** labelled **b** and **b′** outline the terminal cell soma and a branch tip, respectively, and are shown enlarged. Merged images of Crumbs (white) and lumenal membrane (magenta) co-staining are shown. (**c**–**c″**) Subcellular localization of actin relative to the seamless tube is examined. In **c**, a portion of a terminal cell (light-green dots) containing a branched seamless tube (magenta) is shown. In **c′**), the subcellular distribution of actin (Actin::GFP, green) is shown. In **c″**, a merged image is shown. (**d**,**d″**) The white rectangles labelled in **c″** highlight distinct domains of actin localization that are shown enlarged in **d**–**d″**: filopodial actin (**d**), basolateral actin (**d′**) and apical actin (**d″**). Scale bars for **a**,**a′** and for **c**,**c′**,**c″** represent 10 μm, and in **b′** and **d″** for **b**,**b′** and for **d**,**d′**,**d″**, respectively, represent 2 μm.

where they may template tube growth. Consistent with such a role, we observed microtubule-tract-associated fragments of apical membrane distal to the blind ends of the seamless tubes (Fig. 2c–c″, arrow). Filopodia extended past the stable microtubules (Fig. 2e–e″, white arrowhead) as expected. These data indicate that mature terminal cells maintain the polarity and organization described for embryonic terminal cells[7]. On the basis of γ-tubulin localization, we infer that a subset of microtubules is nucleated at the apical membrane, and that apically targeted transport along such microtubules would require minus-end motor proteins. Indeed, homozygous mutant *Lissencephaly-1* (*Lis-1*, a dynein-motor-associated protein) embryos have been reported to have seamless tube defects[7]. As γ-tubulin lines the entire apical membrane, growth through minus-end-directed transport might be expected to occur all along the length of seamless tubes, and indeed, a pulse of CD8::GFP (transmembrane protein tagged with GFP) synthesis uniformly labelled the apical membrane as it first became detectable (Supplementary Fig. S1c,c′ and Supplementary Methods).

The cytoplasmic dynein motor complex drives minus-end-directed transport of intracellular vesicles in many cell types[16]; to test for its requirement in seamless tube formation, we examined terminal cells mutant for any of four dynein motor complex genes: Dynein heavy chain 64C (*Dhc64C*), Dynein light intermediate chain (*dlic*), Dynactin p150 (*Glued*) and *Lis-1*. Mutant terminal cells showed a cell autonomous requirement for these genes. Mutant terminal cells had thin cytoplasmic branches that lacked air-filling (Fig. 3a–e′), and antibody staining revealed that seamless tubes did not extend into these branches although acetylated microtubules often did (Fig. 3f–i and data not shown). We also note that formation of filopodia at branch tips is disrupted in dynein motor complex mutants, which may account for the decreased number of branches in mutant terminal cells. Ectopic seamless tubes that were not air-filled were detected near the nucleus, as described below. Interestingly, discontinuous apical membrane fragments (similar to those in *Lis-1* embryos)[7] were found in terminal branches lacking seamless tubes, and were associated with microtubule tracts (Fig. 3h,i). Whereas γ-tubulin was enriched on truncated tubes and on these presumptive seamless tube intermediates, diffuse γ-tubulin staining was detected throughout the mutant cells (Fig. 3j,j′; compare with Fig. 2a,b), indicating that assembly of apical membrane is required to establish or maintain γ-tubulin localization. Likewise, Crumbs seemed reduced and aberrantly localized (Supplementary Fig. S1d–f). Reduced levels of acetylated microtubule staining in these cells may reflect loss of apical γ-tubulin (compare 3h,i). Importantly, these data show that stable microtubules extend through cellular projections that lack seamless tubes. Thus, without minus-end-directed transport, stable microtubules are insufficient to promote seamless tube formation, but stable cellular projections are formed and maintained in the absence of seamless tubes.

In contrast to these defects in seamless tube generation, mutations in *wkd* (ref. 17) confer overly exuberant tube growth (Fig. 3k,l and Supplementary Fig. S2a,d,i). Examination of *wkd* terminal cell tips revealed a 'U-turn' phenotype in which seamless tubes executed a series of 180° turns—below we entertain the possibility that branch retraction, similar to that observed in talin mutants[18], could contribute to the U-turn defect.

Homozygous *wkd* animals survived until pharate adult stages, and, other than the seamless tube defects, had normal tracheal tubes at the third larval instar. Mosaic analysis revealed a terminal cell autonomous requirement for *wkd*. Mutant clones in multicellular tubes, and in unicellular tubes that lumenize by making autocellular adherens junctions, were of normal morphology (Supplementary Fig. S2f–h). Strikingly, fusion cells, which also form seamless tubes, were unaffected by loss of *wkd*.

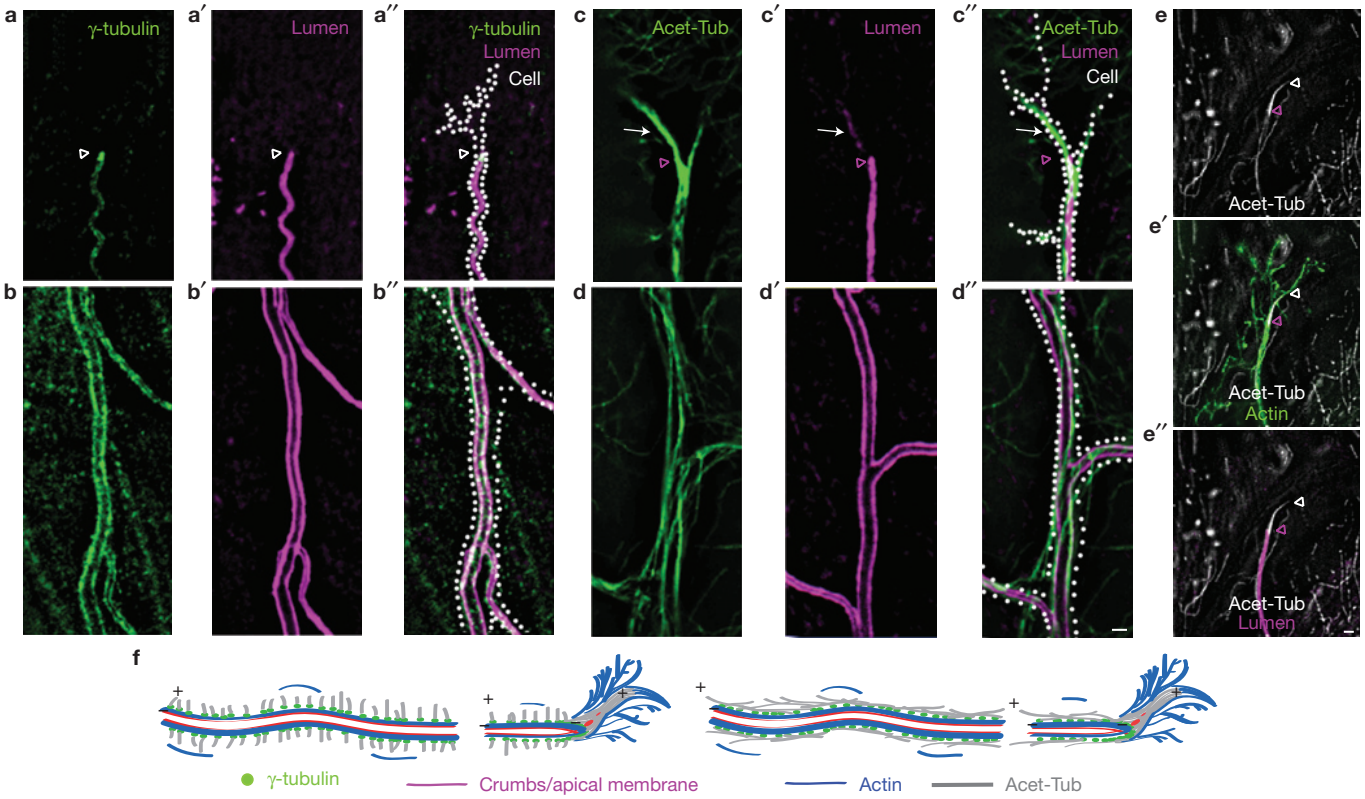

Figure 2 The terminal cell microtubule cytoskeleton is polarized. Terminal cell outlines (determined as in Fig. 1) are indicated (Cell, white dots). (**a**,**b**) The subcellular distribution of γ-tubulin is shown in a typical wild-type terminal cell. γ-tubulin (green) lines the seamless tube and is enriched at the blind end of the tube found at the tip of the terminal cell (**a**). Co-staining of γ-tubulin and apical membrane (magenta, **a**′,**b**′) is shown (**a**″,**b**″). (**c**,**d**) The subcellular distribution of acetylated microtubules (Acet-Tub, green) is shown. Acetylated microtubule bundles run parallel to the apical membrane (magenta, **c**′,**d**′). Co-staining is shown (**c**″,**d**″). We note that apical membrane fragments (white arrow) discontinuous with the seamless tube are found to line acetylated microtubule tracts extending beyond the seamless tube blind end (magenta arrowhead). (**e**) The relationship between acetylated microtubules (white), apical membrane (magenta) and actin-rich filopodia (green) at branch tips is shown. Acetylated microtubules extend beyond (white arrowhead) the blind end (magenta arrowhead) of the seamless tube. Actin-based filopodial projections extend beyond both the seamless tube and the stable microtubule tract. These data (and those from Fig. 1) are summarized in the schematic diagrams shown in **f**. On the left, microtubules are shown oriented perpendicular to the axis of the tube whereas in the panel on the right, microtubules are shown oriented parallel to the long axis of the tube. Either or both microtubule arrangements may be present. Scale bars for **a**–**d** are in **d**″ and for **e**,**e**′, **e**″ are in **e**″ and represent 2 μm.

To determine the molecular nature of *wkd*, we took a positional cloning approach (Supplementary Fig. S3 and Methods). Mapping techniques defined a candidate gene interval of ~75 kilobases (kb). We focused on CG5344 as it encodes a protein containing a TBC (Tre2/Bub2/Cdc16) domain characteristic of Rab GTPase-activating proteins[19–21] (GAPs), and hence was likely to participate in vesicular trafficking, a process that could lie at the heart of seamless tube formation. We identified single nucleotide changes that result in mis-sense (PC24) and non-sense (220) mutations in the CG5344 coding sequence. Pan-tracheal knockdown of *wkd* by RNA-mediated interference (RNAi) caused terminal cell-specific U-turn defects (other defects characteristic of the ethyl methanesulfonate (EMS)-induced alleles of *wkd*—see Supplementary Methods—were detected at a low frequency, data not shown). A genomic rescue construct for CG5344 rescued *wkd* mutants, confirming gene identity (Supplementary Fig. S2j,m). On the basis of these results, we conclude that *wkd* is CG5344 and that it probably regulates vesicular trafficking during seamless tube morphogenesis.

To determine the Rab target(s) of Wkd regulation, we investigated whether tracheal expression of constitutively active 'GTP-locked' Rab isoforms (henceforth, RabCA) might phenocopy *wkd*. RabCA for 31 of the 33 *Drosophila* Rabs[22] were tested individually in the tracheal system. Rab35CA alone conferred terminal-cell-specific U-turns defects (Fig. 4a–g).

To evaluate Wkd overexpression, UAS–*wkd* (Methods) was expressed in wild-type animals in a pan-tracheal pattern. Excess Wkd caused formation of ectopic seamless tubes surrounding the terminal cell nucleus (proximal seamless tube overgrowth; Fig. 4h). At higher levels of expression, small spheres of apical membrane were found adjacent to the nucleus and less abundantly at more distal sites (Supplementary Fig. S4a–l). Consistent with Wkd regulation of vesicle trafficking by modulation of Rab35, expression of a dominant-negative Rab35 (henceforth, Rab35DN) caused formation of ectopic proximal tubules (Fig. 4i,j).

We sought to determine whether Rab35 was the essential target of Wkd GAP activity. Wkd primary structure is equally conserved in three human RabGAPs: TBC1D10C (FLJ00332/Carabin/EPI64C—32% identity), TBC1D10A (EPI64A—30% identity) and TBC1D10B (FLJ13130/EPI64B—27% identity). All three act as Rab35GAPs (ref. 23), although each has been proposed to have additional targets[24–26]. To further determine if Wkd acts as a Rab35GAP, we examined whether Rab35DN could suppress *wkd* mutants; tracheal-specific expression of Rab35DN strongly suppressed the

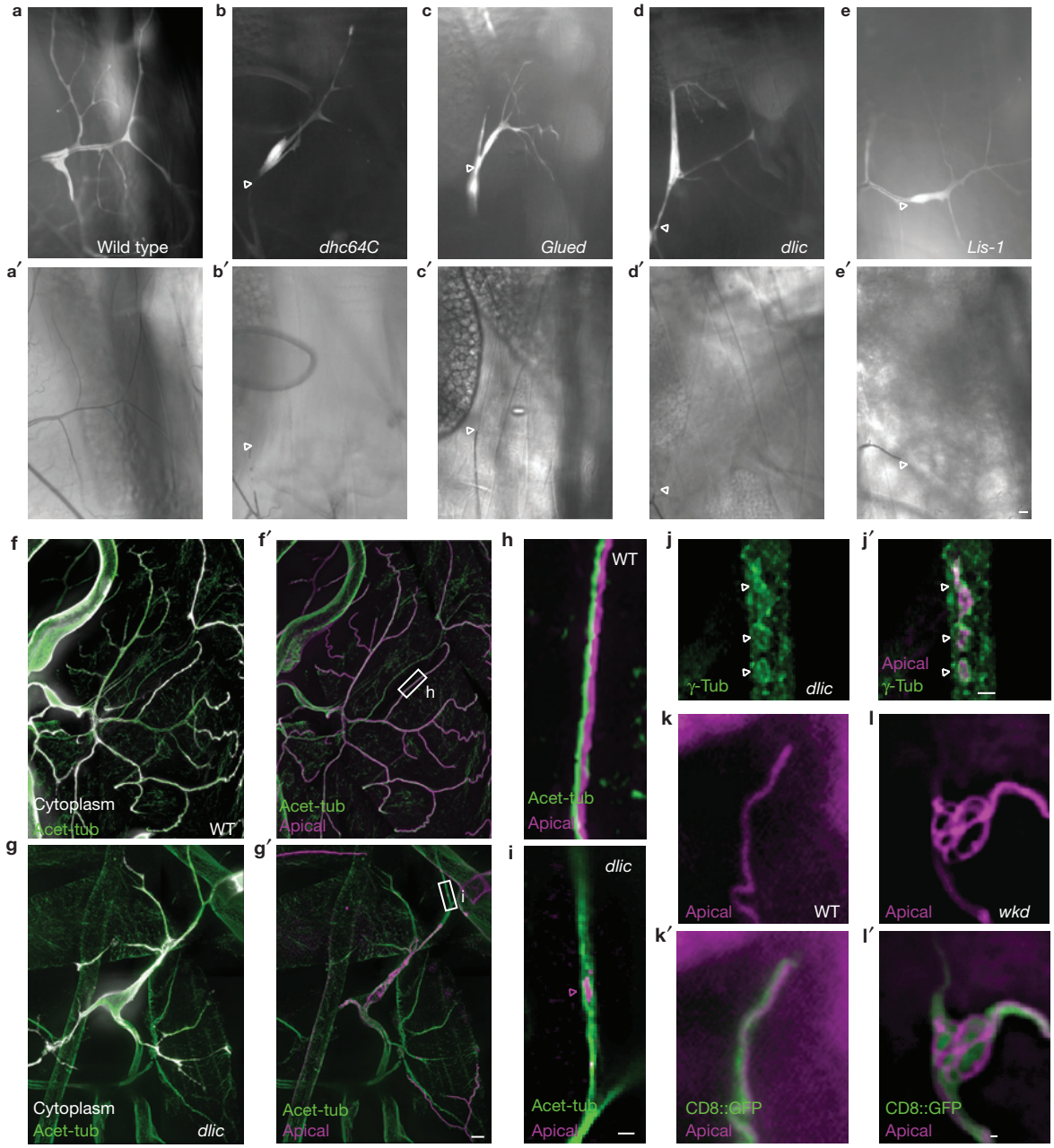

Figure 3 Seamless tube growth is blocked or overly exuberant in dynein motor complex and *wkd* mutants, respectively. (**a**–**d**) Positively marked (GFP, white) mutant terminal cells were identified in mosaic animals. Cells mutant for dynein motor complex components made branched cellular extensions, but had little or no air-filled seamless tubes (arrowheads indicate the position beyond which gas-filling of tubes is not detected, **a**′–**e**′). To determine whether acetylated microtubules (Acet-Tub, green) were present within terminal cells lacking air-filled tubes, wild-type (WT) control (**f**,**f**′) and *dlic* (**g**,**g**′) mosaic animals were filleted, fixed and stained. Homozygous terminal cell clones (**f**,**g**) were marked with GFP (white). Apical membrane (α-Wkdpep, magenta) staining reveals seamless tube remnants near the terminal cell nucleus (**g**′) of mutant terminal cells, but not near branch tips (compare **f**′,**g**′). (**h**,**i**), High-magnification images of seamless tubes from wild-type and *dlic* mutant terminal cells (**f**′,**g**′; outlined area), respectively. In wild type (**h**), continuous seamless tube was present along the acetylated microtubule bundle. In *dlic* mutant cells, apical membrane was absent except for small bits of discontinuous tube that could be detected adjacent to acetylated microtubules (**i**, arrowhead). We found that such discontinuous bits of tube were able to organize γ-tubulin around them, but that γ-tubulin localization was mostly lost in dynein complex mutant terminal cells, with staining present diffusely throughout the cell (**j**,**j**′ compare to Fig. 2a,b). Compared with wild-type animals (**k**,**k**′), seamless tubes in *wkd* terminal cells showed excessive growth at branch tips (**l**,**l**′), resulting in a 'U-turn' phenotype, in which seamless tube extended through the cytoplasm in a series of 180° turns. Scale bars for **a**–**e**′ in **e**′ and for **f**–**g**′ in **g**′ represent 10 μm; for **h**,**i** in **i**, for **j**,**j**′ in **j**′ and for **k**–**l**′ in **l**′ represent 2 μm.

'U-turn' defects of *wkd*-null animals and, surprisingly, also rescued the lethality of *wkd* (Supplementary Fig. S2k,m). As mutant Rab35 isoforms phenocopy *wkd* gain and loss of function, Rab35DN bypasses the requirement for *wkd* and human Wkd orthologues are Rab35GAPs, we conclude that the critical function of Wkd is as a GAP for *Drosophila* Rab35.

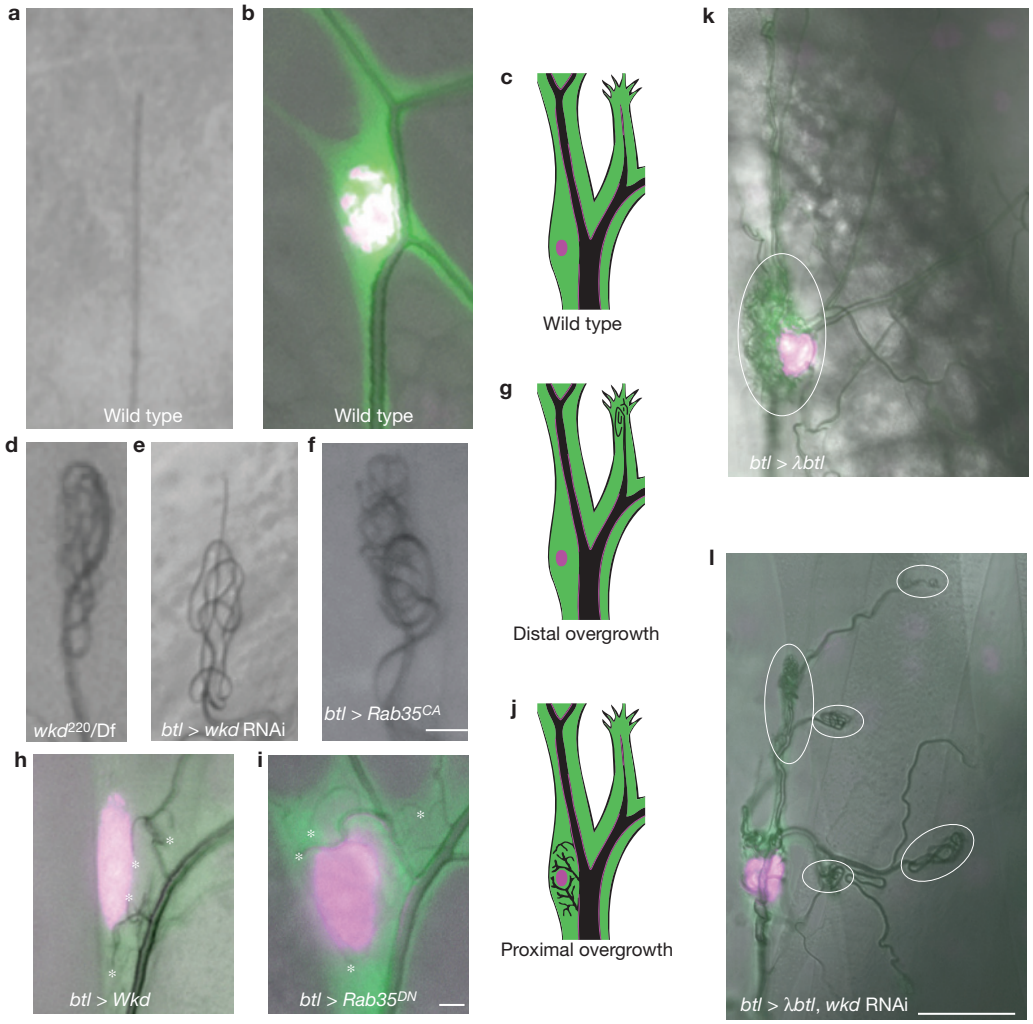

Figure 4 Wkd and Rab35 polarize seamless tube growth. In **a**,**d**–**f**, brightfield micrographs revealing gas-filled terminal cell seamless tubes are shown. In **b**,**h**,**i**,**k** and **l**, fluorescence micrographs labelling the terminal cell cytoplasm (green) and nucleus (magenta) are superimposed on a brightfield image. (**a**,**b**) Wild-type terminal cell branch tip (**a**) and soma (**b**) are shown. (**c**) A schematic illustrates the position and distribution of seamless tubes in wild-type terminal cells. In *wkd* (**d**), *wkd*-RNAi (**e**) or Rab35CA (**f**) terminal cell tips, growth of seamless tubes seems to outpace growth of cellular extensions, resulting in a tangle of gas-filled tubes coiled in the tip cytoplasm. (**g**) The distal seamless tube overgrowth seen in **d**–**f** is illustrated in a schematic diagram. In terminal cells overexpressing Wkd (**h**) or Rab35DN (**i**), ectopic gas-filled seamless tubes (∗) are observed surrounding the terminal cell nucleus. This proximal overgrowth phenotype is illustrated in the schematic in **j**. (**k**) A terminal cell expressing an activated FGFR (λ-*breathless*, λ-btl) produces ectopic gas-filled seamless tubes (outlined with a white oval) surrounding the terminal cell nucleus (magenta), much like (although more extreme than) overexpression of Wkd or Rab35DN. (**l**), A sibling larva expressing a *wkd*-RNAi transgene in addition to λ*btl* shows abundant ectopic tubes (white ovals) at branch tip positions rather than around the nucleus (magenta). Scale bars in **f** (for **a**,**d**–**f**) and **i** (for **b**,**h**,**i**) represent 5 μm, and in **l** (for **l** and **k**) represent 50 μm.

In other systems Rab35 is implicated in polarized membrane addition to plasma membrane compartments—for example, immune synapse, cytokinetic furrow and so on—or, in actin regulation[23,27–36]. A role for actin in fusion cell seamless tube formation has been proposed[37], so we examined whether Wkd and Rab35 act by modulation of the terminal cell actin cytoskeleton. As the actin-bundling protein Fascin (*Drosophila singed*) was recently identified biochemically as a Rab35 effector[36], we tested for a role of *singed* in terminal cell tubes, but found no evidence for one (Methods and Supplementary Fig. S4m–r). Furthermore, overexpression of Wkd (Supplementary Fig. S4t), or of Rab35DN (data not shown), did not significantly alter the terminal cell actin cytoskeleton, leading us to conclude that actin regulation is not a primary function of Wkd/Rab35 during seamless tube morphogenesis.

We found the alternative model—that Rab35 acted in polarized membrane addition—attractive, because extra Rab35-GTP activity promoted seamless tube growth at branch tips whereas depletion of Rab35-GTP promoted tube growth at the cell soma. To test this model, we took advantage of our knowledge that expression of an activated Breathless-FGFR (λ Btl; ref. 38) in terminal cells induces robust growth of ectopic seamless tubes surrounding the nucleus (Fig. 4k and Supplementary Fig. S5a,e); we investigated whether growth of the ectopic tubes could be redirected from the soma to the branch tips by eliminating *wkd*. The activated FGFR phenotype was not altered in *wkd* heterozygotes (Supplementary Fig. S5b,e), but in *wkd* mutant animals (or *wkd*-RNAi animals) the site of ectopic seamless tube growth was strikingly different. In some cells,

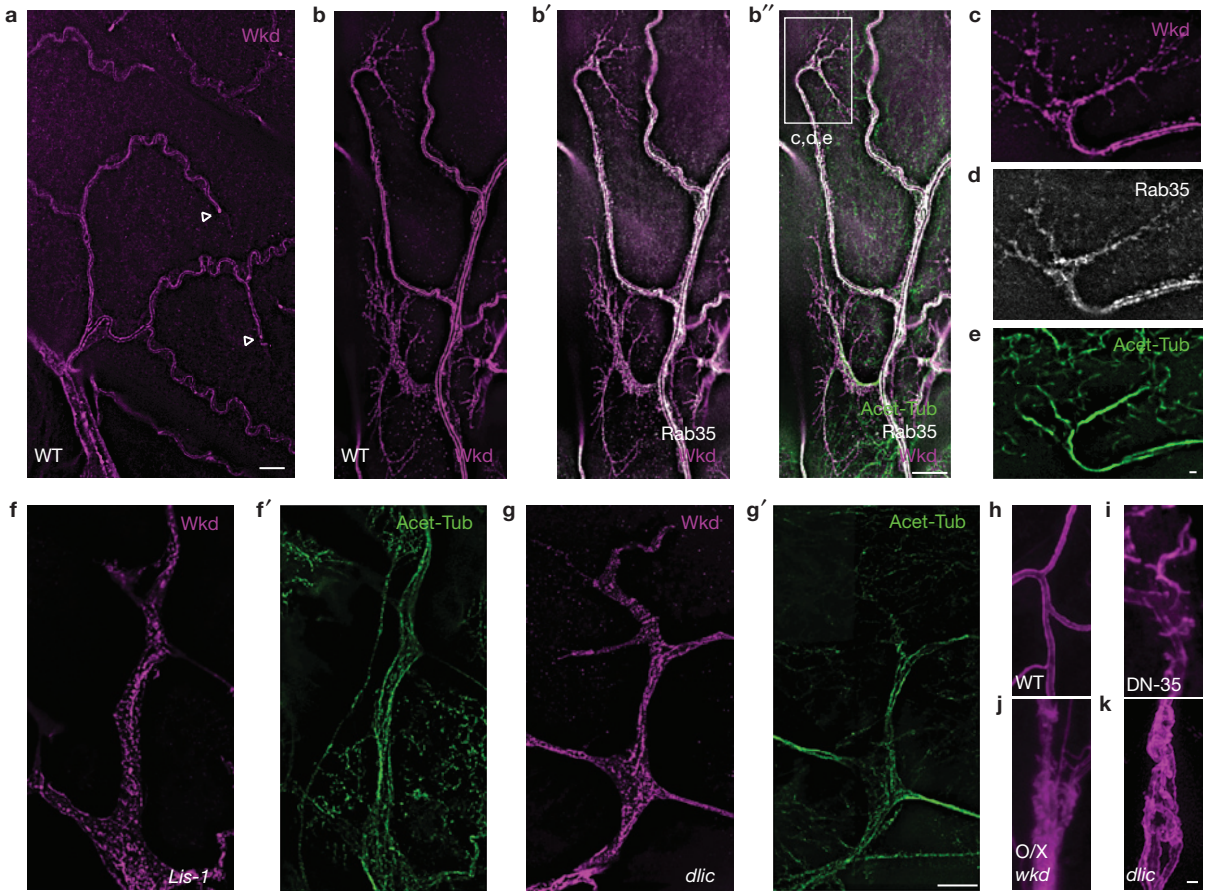

Figure 5 Subcellular distribution of Wkd and Rab35, and the role of minus-end transport in seamless tube growth. (**a**–**e**) In wild-type (WT) terminal cells, Wkd::mKate2 fusion protein (Wkd, magenta) is enriched apically, especially at branch tips (arrowheads). In comparison (**b**′,**b**″,**d**), YFP::Rab35 (white) is more broadly distributed, but also apically enriched. Wkd and Rab35 show extensive co-localization (**b**′), and also overlay with acetylated microtubule tracts (green). At branch tips (outlined area in **b**″), Wkd (**c**) and Rab35 (**d**) are adjacent to acetylated microtubules (**e**), but also decorate actin-based filopodial processes (see Supplementary Fig. S3). In dynein motor complex mutants (*Lis-1*, **f**,**f**′; *dlic* **g**,**g**′), Wkd is dispersed throughout the cytoplasm and often detected on basolateral membrane. Although not excluded from areas with acetylated microtubule bundles, Wkd is not enriched along them (**f**″,**g**″). (**h**–**k**) α-Wkdpep is used to stain the apical membrane of seamless tubes; in the soma surrounding the terminal cell nucleus of wild-type cells (**h**), single seamless tubes are found growing into each cytoplasmic extension, whereas terminal cells expressing a Rab35DN (DN-35) isoform (**i**), overexpressing (O/X) wild-type Wkd (**j**) or mutant for dynein motor complex components such as *dlic* (**k**) have ectopic seamless tubes. Scale bars in **a** for **a**, in **b**″ for **b**–**b**″, and in **g**′ for **f**–**g**′, represent 10 μm; in **e** for **c**–**e** represent 1 μm; and in **k** for **h**–**k** represent 2 μm.

extra tubes were found throughout the cell (Supplementary Fig. S5d,e)—in the soma and at branch tips—whereas in others extra tubes were present only at the branch tip (Fig. 4l and Supplementary Fig. S5c,e). Thus, the position of seamless tube growth is dependent on Wkd activity, although Wkd itself is not essential for tube formation. These data provide evidence against branch retraction (as occurs in talin mutants)[18] as the mechanism for generating a U-turn phenotype, because branch retraction would not redirect ectopic tube growth.

To better understand how Wkd and Rab35 determined the site of seamless tube growth, we investigated their subcellular distribution. Pan-tracheal expression of mKate2-tagged Wkd (Wkd::mKate2) rescued *wkd*-null animals (Supplementary Fig. S2l,m). The steady-state subcellular localization of Wkd::mKate2 was restricted to the lumenal membrane with higher accumulation at the growing tips of seamless tubes (direct fluorescence microscopy of Wkd::mKate2 in a fixed larva, Fig. 5a). At lower levels, we noted cytoplasmic puncta of Wkd::mKate2 that could reflect vesicular localization, and labelling of filopodia (immunofluorescence microscopy using an antibody against mKate2; Fig. 5b,c). We found that YFP::Rab35 was distributed in a diffuse pattern throughout the terminal cell cytoplasm with some apical enrichment, and notable localization to filopodia (Fig. 5b′,d). We find substantial co-localization of Wkd::mKate2 with YFP::Rab35 at the apical membrane, in cytoplasmic puncta, and in filopodia (Fig. 5b″). Among endosomal Rabs, Rab35 seemed uniquely abundant within filopodia, and showed the greatest overlap with Wkd at the apical membrane (Supplementary Fig. S4u–x). We noted substantial overlap between Wkd/Rab35 and acetylated microtubules, including at positions distal to the blind end of seamless tubes (Fig. 5b″,c–e). The enrichment of Wkd along seamless tubes indicates that Rab35 functions in an apical membrane trafficking event, leading us to speculate that recycling endosomes at filopodia might be targeted to the growing seamless tube by minus-end motor transport.

In a similar vein, we speculate that vesicles might be transported from the soma towards branch tips in a process regulated by

Wkd and Rab35. Disruption of such transport might explain why overexpression of Wkd leads to ectopic seamless tube growth in the soma. We examined whether Wkd::mKate2 localization was compromised in dynein motor complex mutants. As these cells have branches that lack apical membrane/seamless tubes, we anticipated disruption in the localization pattern of Wkd, but wondered whether co-localization with acetylated tubulin would be intact, indicative of a microtubule association independent of dynein motor transport. We find that Wkd::mKate2 is broadly distributed throughout the cytoplasm of dynein motor complex mutants, and does not show enrichment on acetylated microtubule tracts (Fig. 5f,f′,g,g′); indeed, we detected substantial basal enrichment of Wkd::mKate2. If Wkd/Rab35-dependent trafficking of apical vesicles was dynein motor complex dependent, we might expect to see ectopic seamless tubes in the soma of dynein motor complex mutants, similar to those seen with Wkd overexpression or expression of Rab35DN. In fact, we consistently find such ectopic tubes in the dynein motor complex mutants (Fig. 5h–k), consistent with dynein-dependent trafficking of Rab35 vesicles. We cannot rule out the possibility that these defects are due to dynein-dependent processes unrelated to Wkd and Rab35; however, we did test whether the ectopic tubes could be redirected distally by expression of Rab35CA, or elimination of Wkd (Supplementary Fig. S1g–g″,h–h″). The motor complex ectopic tube phenotype could not be altered, indicating that the phenotype does not arise as an indirect consequence of altered Wkd localization or Rab35 activity.

The roles of RabGAP proteins have started to become clear only in recent years. Historically, it has been difficult to determine which Rab proteins are substrates of specific RabGAPs (ref. 39). Tests of *in vitro* GAP activity produced conflicting results, and in some cases did not seem indicative of *in vivo* function[40]. Indeed, the specificity of Carabin (also known as Wkd orthologue TBC1D10C) has been controversial: it was first shown to act as a RasGAP (ref. 24), whereas later studies indicate a Rab35-specific GAP activity[23,30,32]. Our *in vivo* genetic data for *wkd*, together with recent studies characterizing the function of all three human Wkd-like TBC proteins[23] (TBC1D10A-C), make a compelling case that this family of proteins acts as GAPs for Rab35. Furthermore, our study establishes a role for classical vesicle trafficking proteins in seamless tube growth. As seamless tubes, but not multicellular or autocellular tracheal tubes, are affected by mutations in *wkd* and Rab35, our study also establishes an *in vivo* cell-type-specific requirement for trafficking genes in tube morphogenesis.

We conclude that Wkd and Rab35 regulate polarized growth of seamless tubes, and speculate that Wkd and Rab35 direct transport of apical membrane vesicles to the distal tip of terminal cell branches (when equilibrium is shifted towards active Rab35-GTP), or to a central location adjacent to the terminal cell nucleus (when equilibrium is shifted towards inactive Rab35-GDP). Analogous to its previously described roles in targeting vesicles to the immune synapse in T cells, the cytokinetic furrow in *Drosophila* S2 cells and the neuromuscular junction in motor neurons, Rab35 would promote transport of vesicles from a recycling endosome compartment to the apical membrane. We further speculate that Breathless-FGFR activation at branch tips may couple terminal cell branching with seamless tube growth within that new branch (Supplementary Fig. S5f). □

METHODS

Methods and any associated references are available in the online version of the paper at www.nature.com/naturecellbiology

Note: Supplementary Information is available on the Nature Cell Biology website

ACKNOWLEDGEMENTS

The authors would like to acknowledge: D. Willis, a former Stanford undergraduate student who helped with the rough mapping of *wkd*; B. Levi, who helped with the third chromosome screen; and M. Krasnow, in whose laboratory the screen and early phases of these studies were carried out. We also thank J. Zhang and the laboratories of M. Scott and H. Bellen (Baylor College of Medicine, USA) for making RabCA and RabDN stocks available to us before publication, the Engels laboratory for sharing deficiency strains, and M. Metzstein (The University of Utah, USA) for sharing 4x-SRF-GAL4 flies. We thank S. DiNardo, C. Burd, E. Bi and members of the Ghabrial and DiNardo laboratories for fruitful discussions. We thank A. S. Burguete, B. Levi and N. Speck for comments on the manuscript. J.S-R. was supported by NIH training grant 5-T32-HD007516-12 and, subsequently, by an NIH postdoctoral fellowship (NRSA—GM090438-01). A.S.G. gratefully acknowledges support from the University of Pennsylvania and the NIH (1R01GM089782-01A1). This work was supported in part by Basil O'Connor Starter Scholar Research Award Grant No. 5-FY09-43 from the March of Dimes Foundation.

AUTHOR CONTRIBUTIONS

J.S-R. and A.S.G. conceived of and carried out all experiments described here. A.S.G. wrote the manuscript with input from J.S-R. Figures were assembled by J.S-R. and A.S.G.

COMPETING FINANCIAL INTERESTS

The authors declare no competing financial interests.

Published online at www.nature.com/naturecellbiology
Reprints and permissions information is available online at www.nature.com/reprints

1. Samakovlis, C. *et al.* Development of the *Drosophila* tracheal system occurs by a series of morphologically distinct but genetically coupled branching events. *Development* **122,** 1395–1407 (1996).
2. Ribeiro, C., Neumann, M. & Affolter, M. Genetic control of cell intercalation during tracheal morphogenesis in *Drosophila*. *Curr. Biol.* **14,** 2197–2207 (2004).
3. Buechner, M. Tubes and the single *C. elegans* excretory cell. *Trends Cell Biol.* **12,** 479–484 (2002).
4. Bar, T., Guldner, F. H. & Wolff, J. R. 'Seamless' endothelial cells of blood capillaries. *Cell Tissue Res.* **235,** 99–106 (1984).
5. Lubarsky, B. & Krasnow, M. A. Tube morphogenesis: making and shaping biological tubes. *Cell* **112,** 19–28 (2003).
6. Uv, A., Cantera, R. & Samakovlis, C. *Drosophila* tracheal morphogenesis: intricate cellular solutions to basic plumbing problems. *Trends Cell Biol.* **13,** 301–309 (2003).
7. Gervais, L. & Casanova, J. *In vivo* coupling of cell elongation and lumen formation in a single cell. *Curr. Biol.* **20,** 359–366 (2010).
8. Brodu, V., Baffet, A. D., Le Droguen, P. M., Casanova, J. & Guichet, A. A developmentally regulated two-step process generates a noncentrosomal microtubule network in *Drosophila* tracheal cells. *Dev. Cell* **18,** 790–801 (2010).
9. Sutherland, D., Samakovlis, C. & Krasnow, M. A. branchless encodes a *Drosophila* FGF homolog that controls tracheal cell migration and the pattern of branching. *Cell* **87,** 1091–1101 (1996).
10. Ribeiro, C., Ebner, A. & Affolter, M. *In vivo* imaging reveals different cellular functions for FGF and Dpp signaling in tracheal branching morphogenesis. *Dev. Cell* **2,** 677–683 (2002).
11. Jarecki, J., Johnson, E. & Krasnow, M. A. Oxygen regulation of airway branching in *Drosophila* is mediated by branchless FGF. *Cell* **99,** 211–220 (1999).
12. Berry, K. L., Bulow, H. E., Hall, D. H. & Hobert, O. A. *C. elegans* CLIC-like protein required for intracellular tube formation and maintenance. *Science* **302,** 2134–2137 (2003).
13. Ulmasov, B., Bruno, J., Gordon, N., Hartnett, M. E. & Edwards, J. C. Chloride intracellular channel protein-4 functions in angiogenesis by supporting acidification of vacuoles along the intracellular tubulogenic pathway. *Am. J. Pathol.* **174,** 1084–1096 (2009).
14. Grawe, F., Wodarz, A., Lee, B., Knust, E. & Skaer, H. The *Drosophila* genes crumbs and stardust are involved in the biogenesis of adherens junctions. *Development* **122,** 951–959 (1996).
15. Wodarz, A., Hinz, U., Engelbert, M. & Knust, E. Expression of crumbs confers apical character on plasma membrane domains of ectodermal epithelia of *Drosophila*. *Cell* **82,** 67–76 (1995).
16. Waterman-Storer, C. M. *et al.* The interaction between cytoplasmic dynein and dynactin is required for fast axonal transport. *Proc. Natl Acad. Sci. USA* **94,** 12180–12185 (1997).

17. Ghabrial, A. S., Levi, B. P. & Krasnow, M. A. A systematic screen for tube morphogenesis and branching genes in the *Drosophila* tracheal system. *PLoS Genet.* **7,** e1002087 (2011).
18. Levi, B. P., Ghabrial, A. S. & Krasnow, M. A. *Drosophila* talin and integrin genes are required for maintenance of tracheal terminal branches and luminal organization. *Development* **133,** 2383–2393 (2006).
19. Albert, S. & Gallwitz, D. Two new members of a family of Ypt/Rab GTPase activating proteins. Promiscuity of substrate recognition. *J. Biol. Chem.* **274,** 33186–33189 (1999).
20. Albert, S., Will, E. & Gallwitz, D. Identification of the catalytic domains and their functionally critical arginine residues of two yeast GTPase-activating proteins specific for Ypt/Rab transport GTPases. *EMBO J.* **18,** 5216–5225 (1999).
21. Strom, M., Vollmer, P., Tan, T. J. & Gallwitz, D. A yeast GTPase-activating protein that interacts specifically with a member of the Ypt/Rab family. *Nature* **361,** 736–739 (1993).
22. Zhang, J. *et al.* Thirty-one flavors of *Drosophila* rab proteins. *Genetics* **176,** 1307–1322 (2007).
23. Hsu, C. *et al.* Regulation of exosome secretion by Rab35 and its GTPase-activating proteins TBC1D10A-C. *J. Cell Biol.* **189,** 223–232 (2010).
24. Pan, F. *et al.* Feedback inhibition of calcineurin and Ras by a dual inhibitory protein Carabin. *Nature* **445,** 433–436 (2007).
25. Itoh, T. & Fukuda, M. Identification of EPI64 as a GTPase-activating protein specific for Rab27A. *J. Biol. Chem.* **281,** 31823–31831 (2006).
26. Ishibashi, K., Kanno, E., Itoh, T. & Fukuda, M. Identification and characterization of a novel Tre-2/Bub2/Cdc16 (TBC) protein that possesses Rab3A-GAP activity. *Genes Cells* **14,** 41–52 (2009).
27. Chevallier, J. *et al.* Rab35 regulates neurite outgrowth and cell shape. *FEBS Lett.* **583,** 1096–1101 (2009).
28. Chua, C. E., Lim, Y. S. & Tang, B. L. Rab35—a vesicular traffic-regulating small GTPase with actin modulating roles. *FEBS Lett.* **584,** 1–6 (2010).
29. Echard, A. Membrane traffic and polarization of lipid domains during cytokinesis. *Biochem. Soc. Trans.* **36,** 395–399 (2008).
30. Gao, Y. *et al.* Recycling of the Ca^{2+}-activated K^{+} channel, KCa2.3, is dependent upon RME-1, Rab35/EPI64C, and an N-terminal domain. *J. Biol. Chem.* **285,** 17938–17953 (2010).
31. Kouranti, I., Sachse, M., Arouche, N., Goud, B. & Echard, A. Rab35 regulates an endocytic recycling pathway essential for the terminal steps of cytokinesis. *Curr. Biol.* **16,** 1719–1725 (2006).
32. Patino-Lopez, G. *et al.* Rab35 and its GAP EPI64C in T cells regulate receptor recycling and immunological synapse formation. *J. Biol. Chem.* **283,** 18323–18330 (2008).
33. Sato, M. *et al.* Regulation of endocytic recycling by *C. elegans* Rab35 and its regulator RME-4, a coated-pit protein. *EMBO J.* **27,** 1183–1196 (2008).
34. Shim, J. *et al.* Rab35 mediates transport of Cdc42 and Rac1 to the plasma membrane during phagocytosis. *Mol. Cell Biol.* **30,** 1421–1433 (2010).
35. Uytterhoeven, V., Kuenen, S., Kasprowicz, J., Miskiewicz, K. & Verstreken, P. Loss of skywalker reveals synaptic endosomes as sorting stations for synaptic vesicle proteins. *Cell* **145,** 117–132 (2011).
36. Zhang, J., Fonovic, M., Suyama, K., Bogyo, M. & Scott, M. P. Rab35 controls actin bundling by recruiting fascin as an effector protein. *Science* **325,** 1250–1254 (2009).
37. Lee, S. & Kolodziej, P. A. The plakin Short Stop and the RhoA GTPase are required for E-cadherin-dependent apical surface remodeling during tracheal tube fusion. *Development* **129,** 1509–1520 (2002).
38. Lee, T., Hacohen, N., Krasnow, M. & Montell, D. J. Regulated Breathless receptor tyrosine kinase activity required to pattern cell migration and branching in the *Drosophila* tracheal system. *Genes Dev.* **10,** 2912–2921 (1996).
39. Pfeffer, S. Filling the Rab GAP. *Nat. Cell Biol.* **7,** 856–857 (2005).
40. Fuchs, E. *et al.* Specific Rab GTPase-activating proteins define the Shiga toxin and epidermal growth factor uptake pathways. *J. Cell Biol.* **177,** 1133–1143 (2007).

METHODS

Fly strains. EMS alleles of *wkd* were generated elsewhere[17] and are characterized below. The *Minos* allele of *wkd* (http://flybase.org) is available from the Bloomington Stock Center (http://flystocks.bio.indiana.edu). Mosaic analyses: FRT82B, wkd^{220}, FRTG13, $Lis1^{G10.14}$; $Dhc64C^{4-19}$, FRT2A; $Glued^{1}$, FRT2A; and $dlic^{1}$ and $dlic^{2}$ FRT19A (provided by T. Uemura, Kyoto University, Japan). Alleles of *singed* used sn^{36a}, sn^{X2} and Df(1)c128. UAS–*YFP::Rab* (wild type, CA and DN) strains were a gift from J. Zhang (Stanford University, USA) and M. Scott[22] (Stanford University, USA). The UAS–*wkd*-RNAi strain was obtained from the VDRC (http://stockcenter.vdrc.at/control/main). UAS–λ*btl* has been described previously[38], and a second chromosome insertion was generated (A.S.G.) by *P*-element mobilization. *crumbs*::GFP was a gift from Y. Hong[41] (University of Pittsburgh School of Medicine, USA). UAS–*wkd* was generated by digesting *wkd* complementary DNA RE26521 (DGRC) with XhoI and BamH1 and ligating to pUAST cut with XhoI and partially digested with BamH1. Orientation of the insert was confirmed by testing for the presence of the EcoR1 site in the pUAST polylinker. For Wkd::mKate2 fusion, the *wkd* cDNA was subcloned into pKS-bluescript, and an NcoI site was introduced in place of the *wkd* stop codon. pmKate2 (Evrogen) was digested with NcoI and Not I, and inserted, in frame, downstream of the *wkd* coding sequence. The *wkd::mKate2* fusion was cloned into pUAST. For the *wkd* genomic rescue construct, a 3,909-base-pair (bp) PCR product was amplified from a w^{1118} genomic DNA (Qiagen DNeasy Kit) template using Phusion high-fidelity DNA polymerase (New England Biolabs). The PCR product was cloned using a TopoTA cloning kit (Invitrogen). Clones were sequenced and mutant-free DNA was excised from the pCRII-Topo with KpnI, and placed into pCasper4. UAS and genomic constructs were injected to generate transgenic strains according to standard protocols[42], or by Genetic Services. pWG9.2, a second chromosome insertion of the *wkd* genomic DNA construct, rescued the tracheal defects and lethality associated with wkd^{220}/Df(3R)Exel6276 and wkd^{MINOS}/Df(3R)Exel6276 flies. Deficiency strains (http://flybase.org) are available from the Bloomington Stock Center, except for Df(3R)pros235, Df(3R)pros640 and Df(3R) thoRI, which were gifts from the Engels laboratory.

***wkd* alleles.** Although the U-turn phenotype is the predominant defect in *wkd* mutant animals, in our initial characterization of *wkd* we found that terminal cell seamless tubes often came to premature dead-ends (similar to the dynein motor mutants), and that the overall number of branches in each terminal cell was reduced[17] (Supplementary Fig. S2). Truncated tubes terminated in irregular shapes, leading us to name the gene *wkd*, to reflect the appearance that tubes had been crudely lopped off. However, extensive outcrossing of the wkd^{220} strain resulted in a simplified phenotype in which a robust U-turn defect persisted but all other tube and branching defects were greatly reduced in frequency—this indicates that the principle phenotype of *wkd* mutants is exuberant seamless tube growth at branch tips, and also that loss of *wkd* sensitizes formation of seamless tubes to genetic background. Interestingly, these other phenotypes were also rescued by the *wkd* genomic rescue construct (see below).

Positional cloning. Meiotic recombination placed *wkd* in the interval defined by the recessive markers *curled* (*cu*) and *stripe* (*sr*). Complementation tests against deficiency strains spanning the interval between *cu* and *sr* showed that *wkd* was uncovered by Df(3R)MKX1, which deletes polytene bands 86C1 to 87B1-5. Recombinant chromosomes in which crossovers occurred between *cu* and *sr* were typed with various RFLP SNP markers including 86E5 and 86F10 that defined a smaller (∼300 kb) candidate interval for *wkd*. Strains with small defined chromosomal deletions spanning 86E to 86F10 were tested for complementation, establishing a ∼75 kb segment of the chromosome in 86E14-17 as the location of the *wkd* gene.

Primers. *wkd* genomic rescue construct: forward genomic primer 5′-GGTACC CGTAAACTTGAACGTTGCCACC-3′ and reverse genomic primer 5′-GGTACCGGTCTATGCACGTGAGCG-3′. RFLP snp mapping—86E5 (MspI: 2FRT parental chromosome is uncut, but the *ru h th st cu sr e ca* chromosome is cut). pros1507F: 5′-CCACCAAACTTCGGAATGCC-3′; pros2235B: 5′-TGGGGGTCGCTTATGCTTAGAC-3′; 86F10 (NlaIV: 2FRT parental chromosome is cut, but the *ru h th st cu sr e ca* chromosome is uncut). 86F10F: 5′-ATTACGATGCCTTCGGTCCAC-3′; 86F10B: 5′-AATGTCCTCACTTGTGCCACTG-3′. *wkd* transcription unit sequence analysis: TBC1F: 5′-TGCCACCTGGTTTTTGCTCTAC-3′; TBC1B: 5′-CGAATGGGGGAA-ATCTCAATG-3′; TBC2F: 5′-TTTCACTGTCCCATTCCGTTTG-3′; TBC2B: 5′-ATGTAGAGCCACTTCTTCTCCCGC-3′; TBC3F: 5′-CGAAATGGCTTCTATG-GCGG-3′; TBC3B: 5′-TTCTTCAGCAGACCCTCCAGGATG-3′; TBC4F: 5′-GTCAGCGTGTGCGATGTGTAAG-3′; TBC4B: 5′-TGAACCAGTTTTGGGGT-CACTC-3′; TBC5F: 5′-AAGGTGGCTCTGGTCATTATTGG-3′; TBC5B: 5′-AAACTTTTCAGGCTCGGGGG-3′; TBC6F: 5′-ATGATTACCACCCTGAGG-CAGC-3′; TBC6B: 5′-TTTGGACGATGATGGCGACG-3′.

Sequence analyses. *wkd* DNA and control DNA from the parental strain on which *wkd* mutations were induced, were amplified by PCR and sequenced. In DNA from wkd^{PC24} homozygous animals, a single nucleotide change from the parental chromosome was detected that corresponded to a T-to-A transversion, a mis-sense mutation causing an amino-acid substitution in the conserved TBC domain of Wkd. In DNA from wkd^{220} animals, a C-to-T transition was detected, resulting in a non-sense mutation at the sixth codon position in the *wkd* coding sequence. Further support for the identity of *wkd* came from the subsequent identification of a third mutant allele, this one generated by the insertion of a Minos transposable element into the coding sequence of CG5344 (ref. 43). Terminal cells mutant for the Minos allele of *wkd* exhibited a decreased number of branches and the U-turn phenotype.

Immunohistochemistry. Antibodies used in these studies include: mouse α-mRFP (1:1,000, Abcam ab65856-100), rabbit α-tRFP (anti-mKate2, 1:2,000, Evrogen AB234), chick α-GFP (1:1,000, Invitrogen A10262), mouse α-acetylated-tubulin monoclonal antibody (1:2,000, Sigma T6793), mouse α–γ-tubulin monoclonal antibody (1:1,000, GTU-88, Sigma T6557). The Wkdpep rabbit polyclonal antibody was generated against the Wkd peptide, EHTRQKARRAKQKAQQE, but is used as a marker of terminal cell lumenal membrane. Serum is not specific for Wkd as lumenal membrane staining is still detected in *wkd*-null (220/Df) and wkd^{MINOS} larvae (the Minos insertion is within the last *wkd* exon, 5′ of the nucleotides coding for the Wkd peptide antigen). DsRed, GFP and mKate2 were visualized by direct fluorescence microscopy in heat-killed or fixed larvae, or by antibody staining of fixed and filleted larvae.

Fascin and Egalitarian studies. We carried out tests to determine whether *singed* might be the essential Rab35 effector in tracheal terminal cells for seamless tube morphogenesis. First, we investigated whether terminal cells lacking Fascin exhibited defects consistent with loss of Rab35 activity. We found that *singed*-null terminal cells were entirely wild type in appearance (Supplementary Fig. S5b). Loss of *singed* also did not suppress the *wkd* mutant phenotype (Supplementary Fig. S5c,d). Likewise, loss of *singed* showed no apparent alteration of actin organization in terminal cells (Supplementary Fig. S5f,j). Furthermore, overexpression of Wkd (Supplementary Fig. S5h,i), or Rab35DN (data not shown), did not alter the terminal cell actin cytoskeleton, leading us to conclude that actin regulation is not a primary function of Wkd/Rab35 during seamless tube morphogenesis.

To test for a requirement for *egalitarian*, which serves as an adaptor for apically localized messenger RNA transport, we examined third-instar larvae homozygous for egl^{1}. Mutant terminal cells were indistinguishable from wild type (data not shown); however, we cannot rule out the possibility that maternal *egl* mRNA and protein masked a requirement for Egl function in seamless tube formation.

Double-mutant analyses. The following crosses were carried out: *btl–GAL4*, UAS–*GFP*; wkd^{220}/TM3Sb, TubGal80 flies were crossed with UAS–λ*btl*/CyO, UAS–*DsRed*; Df(3R)EXEL/TM6B, UAS–*DsRed*, or with UAS–*Rab35DN*/CyO, UAS–*DsRed*; Df(3R)EXEL/TM6B, UAS–*DsRed*. The progeny of these crosses that lacked DsRed expression were the experimental genotype, and sibling DsRed-expressing larvae that lacked the Tubby phenotype served as *wkd* loss-of-function controls. The *sn* and *wkd* double-mutant analysis was carried out as follows: Df(1)c128/FM7aGFP; Df(3R)EXEL6276/TM6B females were crossed to $singed^{X2}$; wkd^{MI}/TM6B males. The experimental genotypes were those progeny that lacked GFP and Tubby, and female siblings expressing GFP but lacking Tubby were used as *wkd* loss-of-function controls. To generate tracheal cells deficient for *dlic* and*wkd*, $dlic^{1}$/FM7; wkd^{220}/+ females were crossed to UAS–*GFP* RNAi, FRT19A FLP^{122}; *btl–GAL4*, UAS–*GFP*; Df(3R)EXEL6276/+ males and progeny were heat shocked at 38.5 °C for 1 h after a 4 h egg collection. The $wkd^{220/Df}$ progeny were identified by their tracheal phenotype and were screened for *dlic* clones (GFP positive). To generate animals in which constitutively active Rab35 was expressed in *dlic* mutant terminal cells, $dlic^{1}$/FM7; UAS–*Rab35CA* females were crossed to TubGal80 FRT19A FLP^{122}; *btl–GAL4* UAS–*GFP* males and the progeny were heat shocked at 38.5 °C for 1 h after a 4 h egg collection. Positively marked clones were identified and scored for phenotype.

Pulsed CD8::GFP experiment. TubGal80ts flies were crossed with *btl–GAL4*, UAS–*CD8::GFP* flies, and the larvae were maintained at 18 °C until the third larval instar. Larvae were then subjected to 1 h heat shock at 38.5 °C to inactivate Gal80 and allow for *btl–GAL4*-driven expression of CD8::GFP. Larvae were filleted, fixed and stained (as described in the Methods) at 1, 2 and 3 h after the temperature shift.

Transgene rescue of *wkd* viability. The following crosses were carried out. *Rab35DN*: UAS–*Rab35DN*; Df(3R)EXEL6276/TM6B X *btl–GAL4>DsRed*/CyO; wkd^{220}/TM6B. Genomic rescue: genomic rescue/S; Df(3R)EXEL6276/TM6B

DOI: 10.1038/ncb2454

males were crossed to virgins that were *btl–GAL4 > DsRed*/CyO; wkd^{220}/TM6B. Wkd::mKate2: *btl–Gal4* > wkd :: mkate2/CyO; Df(3R)EXEL6276/MKRS X *Sp*/CyO; wkd^{220}/MKRS. Adults with the rescuing transgenes were scored.

Live imaging of EB1::GFP in the larval tracheal system. Third-instar larvae of the genotype 4x-SRF–GAL4, UAS–EB1GFP were anaesthetized with ether for 15 min and imaged for up to 20 min on an Olympus spinning-disc confocal microscope. Images were acquired with a ×60, 1.2 NA UPlanApo water-immersion objective on a spinning-disc confocal set-up consisting of a Yokogawa CSU-X1 confocal scanner attached to an Olympus IX-81 microscope. The camera was an Andor iXon3 EMCCD camera and acquisition was controlled by MetaMorph 7.7. Images were collected at 2 frames s^{-1} for 1 min. Direction of EB1 movement was determined by manual tracking of GFP fluorescence signal over a 10–20 s interval.

41. Huang, J., Zhou, W., Dong, W., Watson, A. M. & Hong, Y. Directed, efficient, and versatile modifications of the *Drosophila* genome by genomic engineering. *Proc. Natl Acad. Sci. USA* **106,** 8284–8289 (2009).
42. Rubin, G. M. & Spradling, A. C. Genetic transformation of *Drosophila* with transposable element vectors. *Science* **218,** 348–353 (1982).
43. Bellen, H. J. *et al.* The BDGP gene disruption project: single transposon insertions associated with 40% of *Drosophila* genes. *Genetics* **167,** 761–781 (2004).

nature cell biology

DOI: 10.1038/ncb2454

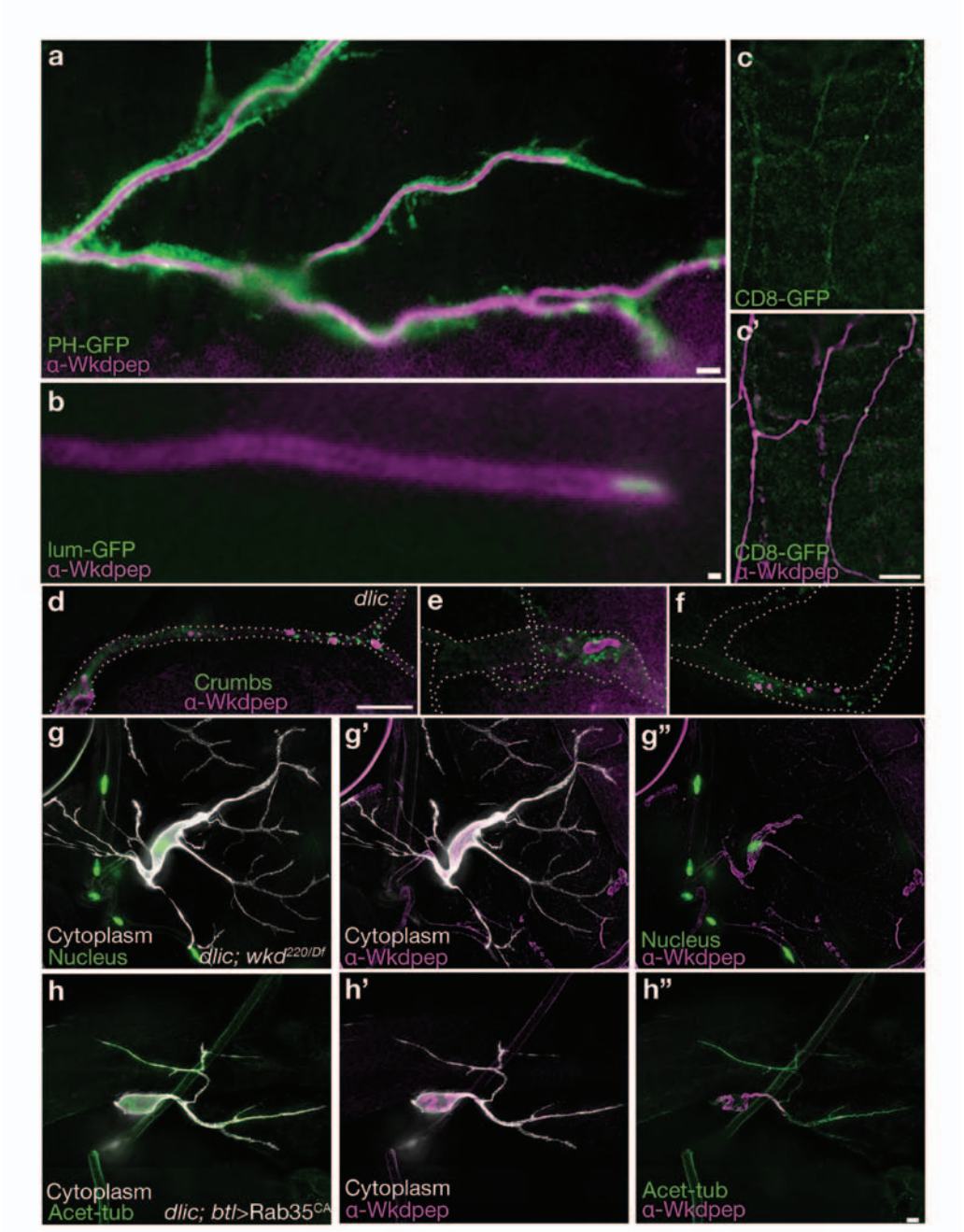

Figure S1 The α-Wkdpep sera recognizes a lumenal membrane associated antigen and highlights defects in seamless tube formation in *dlic* mutants. In all panels, staining with the Rabbit α-Wkdpep sera is shown in magenta. In (a) PH-GFP (green) highlights the terminal cell branch outline and filopodia. Scale bar = 10 microns. In (b) lum-GFP [17] accumulates in the liquid-filled tip of a terminal cell tube. Note that the α-Wkdpep staining surrounds the lum-GFP, but is excluded from the lumen of the tube. Scale bar = 2 microns. In (c, c') a terminal cell from a tubGal80ts; btl-Gal4, UAS-CD8::GFP larvae is shown (CD8::GFP, green). Expression of CD8::GFP was induced by temperature shift in the third larval instar. After 3 hrs, the larvae was filleted, fixed, and stained. Note that CD8::GFP is detectable at low levels throughout the terminal cell, while scattered bright puncta of staining may represent newly added CD8::GFP that has not mixed by lateral diffusion. (d-f) Endogenous Crumbs::GFP (green) expression in three *dlic* mutant terminal cells. Crumbs localizes to rudimentary tubes in the soma of *dlic* mutants (d) but does not consistently overlap with discontinuous pieces of tube found more distally (d-f). Crumbs expression around tube fragments was often patchy (e) and could also be observed in regions devoid of our lumenal membrane marker (f). Cell shape is outlined by a white-dotted line (traced from a captured image showing expression of cytoplasmic DsRed). Scale bar = 10 microns. Seamless tube defects in *dlic* mutants are not the result of Whacked mislocalization. (g-g") A terminal cell double mutant for *dlic* and *whacked*. Double mutant cells are indistinguishable from *dlic* mutants alone (compare to Figure 2g and 2g'). Moreover, tracheal expression of constitutively active Rab35 is not sufficient to rescue the *dlic* mutant phenotype (h-h"). cytoplasmic GFP in white, nuclear DsRed or acetylated-tubulin in green. Scale bar = 10 microns.

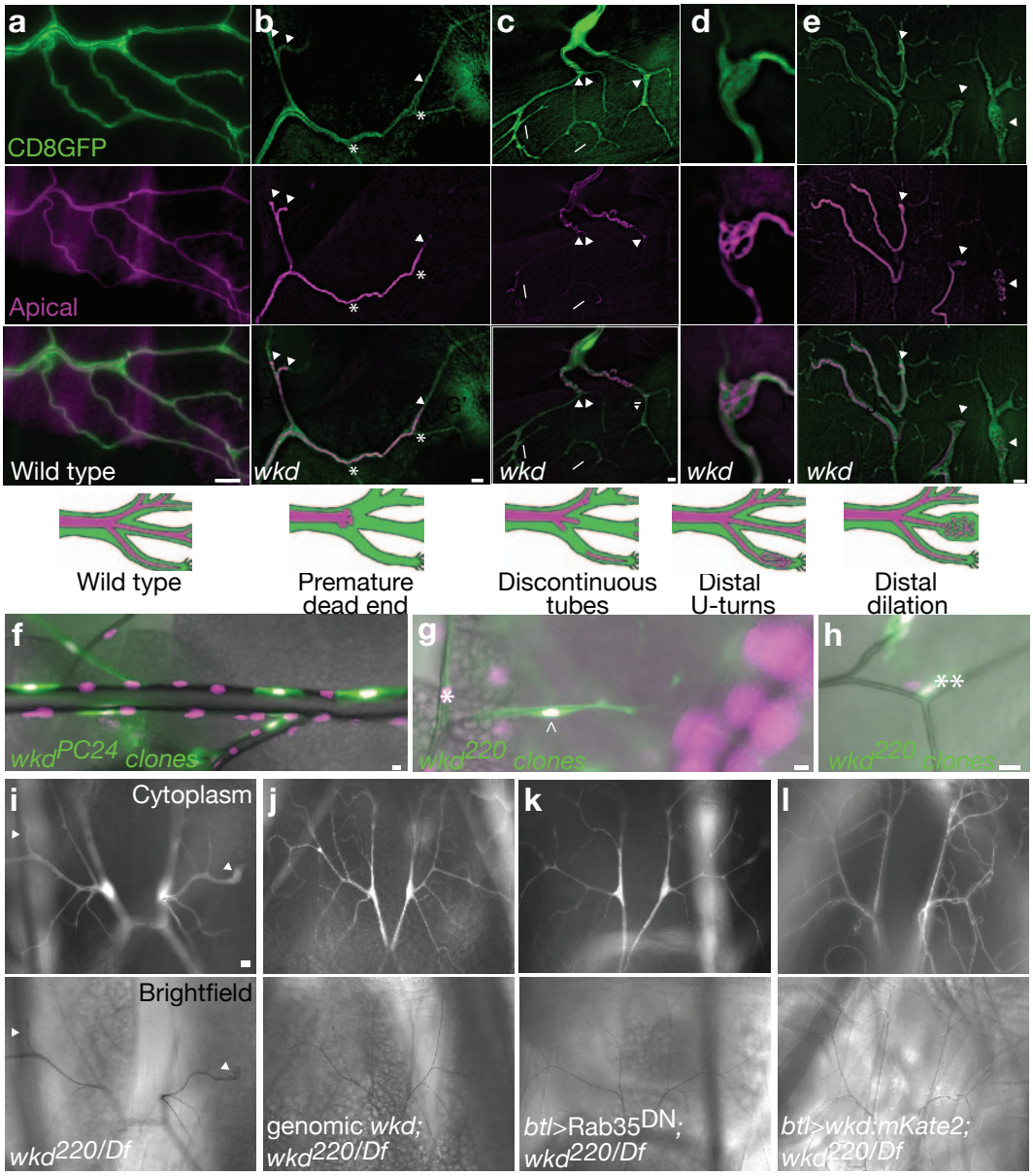

m

Genotype	*n*	Trachea: Distal OG* (%)	Trachea: Wt (%)	Trachea: Proximal OG* (%)	*n*	Viability: Expected (%)	Viability: Observed (%)
wkd$^{220/Df}$	85	65	35	0			
Genomic *wkd*; *wkd*$^{220/Df}$	96	0	100	0	96	25	29
btl>*wkd:mKate2*; *wkd*$^{220/Df}$	16	0	100	0	39	25	29
btl>Rab35^{CA}; *wkd*$^{220/Df}$	64	2	69	29	75	20	28

Figure S2 *whacked* encodes a RabGAP protein. Meiotic recombination mapping (a) placed *whacked* into the interval defined by the recessive markers *curled* (*cu*) and *stripe* (*sr*). Complementation tests against chromosomal deficiency strains further refined the map position of *whacked*, although anomalous results were obtained with Df(3R)T-32 and T-61. The use of SNP markers (see M&M) verified and further refined the *whacked* candidate gene interval (b), and a series of small overlapping chromosomal deficiency strains with molecularly defined breakpoints were used to identify a final candidate interval of ~ 78 kb. Sequence analysis revealed that *whacked* corresponds to the predicted gene CG5344, with each allele of *whacked* showing a single nucleotide change, as compared to parental DNA, resulting in mis-sense and nonsense changes in the coding sequence. In (c), a schematic of the predicted 363 amino acid Whacked protein, with a central TBC domain, is shown. Mutations in the 220 and PC24 alleles are predicted to truncate the protein prior to the TBC domain, or to alter the TBC domain, respectively. In (d), a ClustalW alignment of Whacked, its three human homologues, and the TBC consensus sequence is shown. Alignment reveals high sequence similarity within the putative RabGAP domain, and conservation of the invariant "dual finger" R and Q residues (indicated in red); position of the M to K mutation in PC24 is indicated (K in green).

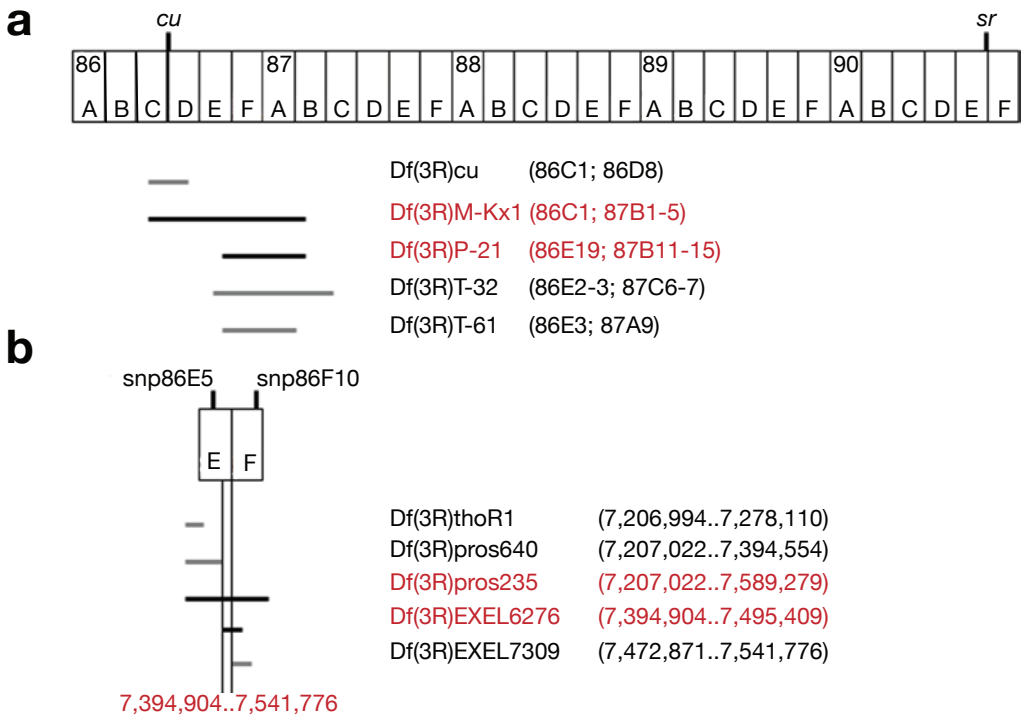

Figure S3 Only seamless tubes are defective in *whacked* mutant animals. In (a-e), the terminal cell is marked by CD8-GFP (green) and the seamless tubes running through the cells are visualized by staining against α-Wkdpep (magenta). Merged images (lower middle panels) and schematic drawings illustrating the phenotypes (bottom panels). (a) wild type and (b-e) *whacked*$^{220/Df}$ mutant terminal cells. In (b), a portion of a *whacked* mutant terminal cell is shown; note the presence of fewer side branches, and that tube lumens are prematurely truncated (arrowheads); some branches of the terminal cell (*) completely lack lumens. In another *whacked* terminal cell (c), the seamless tubes within the terminal branches are discontinuous (arrowheads indicate deadends of proximal tubes and arrows indicate start of distal tubes). In (d, same as Figure 3i), a high magnification view of the tip of a *whacked* terminal cell branch reveals a tangled tube that appears to execute a series of U-turns within the branch tip cytoplasm. In other *whacked* terminal cells (e), distal dilations in a terminal branches are observed (arrowheads), in which the associated seamless tube looks highly irregular and rough in appearance. In f – h, a mosaic analysis of whacked is shown in which homozygous mutant cells are labeled with GFP and all tracheal nuclei are marked with DsRED2nls (magenta). The fluorescent images are superimposed on brightfield images that allow assessment of gas-filling. Dorsal trunk clones (f), stalk cell clones (g, *), and fusion cell clones (h, **) appear normal but terminal cell clones (g, ^) show the spectrum of defects described above. Bars: a – c, e – 5 microns; d – 1 micron. f – h, 10 microns. (i-l) Third-instar larval terminal cells mutant for *whacked*$^{220/Df}$ display an overgrowth of seamless tube at the distal tips of terminal branches (i, arrowheads) and a reduction in the number of branches. These defects can be rescued or suppressed by addition of a *whacked* genomic rescue construct (j), tracheal expression of Rab35^{DN} (k), or tracheal expression of Wkd::mKate2 (l). Scale bar = 10 microns. (m) Table of *whacked* mutant rescue data. *OG = overgrowth

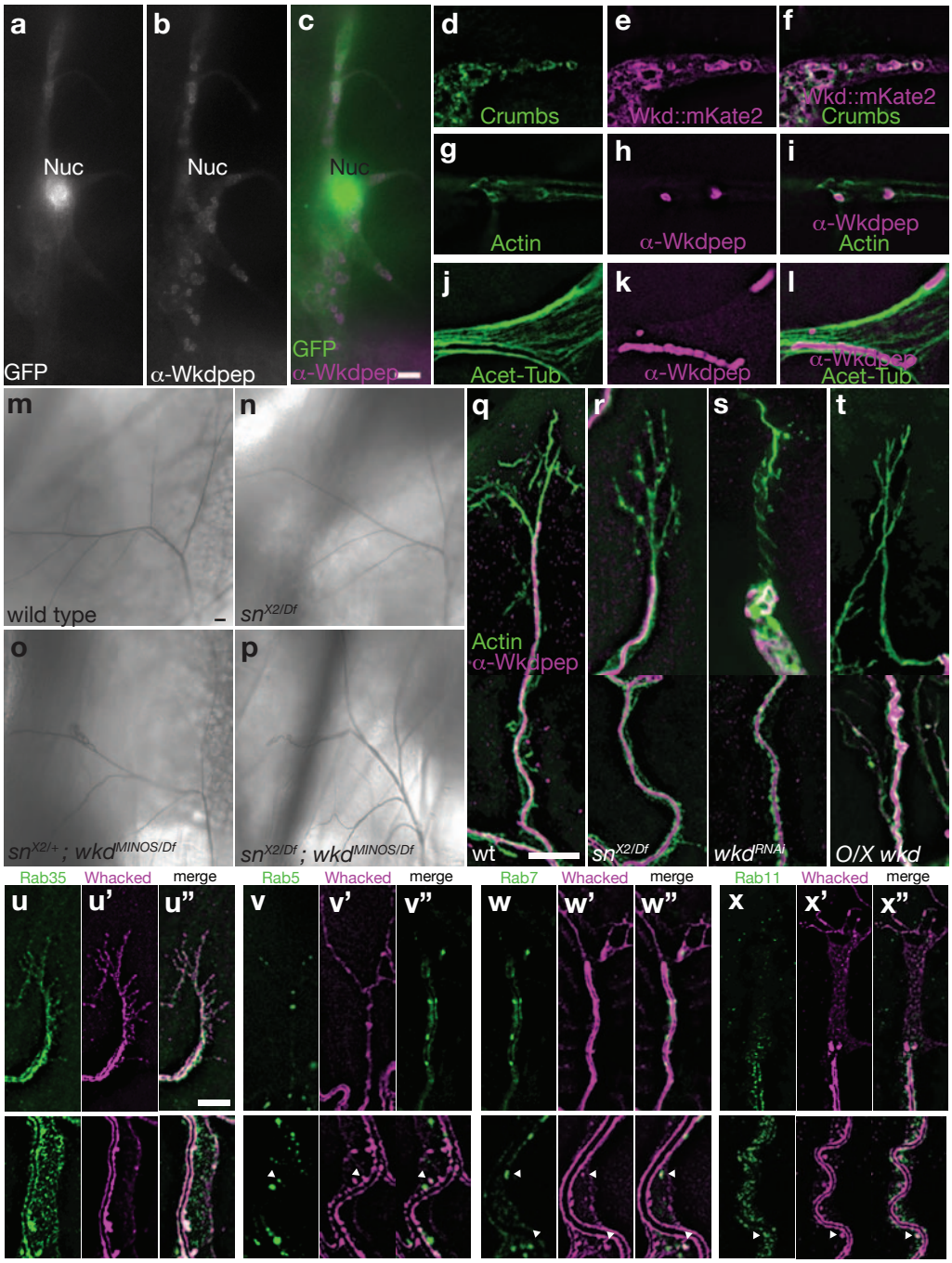

Figure S4 Whacked and Rab35 localize to filopodia, but do not appear to influence actin dynamics in terminal cells. (a-c) Gross overexpression of UAS-*wkd* in the tracheal system leads to the production of discontinuous membrane spheres in terminal cells at the expense of gas-filled tubes (cytoplasmic GFP - white (a) green (c), α-Wkdpep - white (b) magenta (c)). These ectopic spheres have apical identity as revealed by co-localization with Crumbs::GFP (green, d-f) and the ability to recruit actin (green, g-i). (j-l) These cells often showed discontinuous pieces of tube associated with microtubule tracts, similar to what we see with dynein motor complex mutants (acetylated microtubules, green). (m-p) Fascin is not the critical effector of Rab35 in tracheal terminal cells. Terminal cells mutant for *singed* (n) are morphologically indistinguishable from wildtype (m). Terminal cells mutant for *whacked*$^{lMINOS/Df}$ and heterozygous (o) or mutant for *singed* (p) were indistinguishable from *whacked* mutants alone. Furthermore, no obvious defects in apical and filopodial localization of actin in terminal cells of *sn* and *whacked* mutants exists (q-r, branch tips top panels, more proximal positions bottom panels). Although *wkd* RNAi and Wkd overexpression (O/X) cause tube defects, actin is localized to the apical membrane of these tubes (s, t - bottom) and filopodia still decorate the tips of branches (s, t - top). However, the filopodia in *wkd* mutants (data not shown) and *wkd* RNAi (s) are frequently less branched than wild type (q). (u-x) Analysis of endocytic Rab::Wkd co-localization (immunostaining against mKate2 and YFP) at seamless tubes and in filopodial processes. Rab35 (u) is uniquely enriched in filopodia (top panels) and broadly co-localizes with Wkd (u') at seamless tubes (bottom panels). Only small amounts of Rab5 (early endosome, v), Rab7 (late endosome, w) and Rab11 (recycling endosome, x) localize with Wkd in filopodia, highlighting a unique relationship between Rab35 and Wkd at the distal tips of branches. Puncta of Wkd do occasionally co-localize (arrowheads) with Rab5, Rab7, and Rab11 along seamless tubes (bottom panels). Scale bar = 10 microns (m-t) and 5 microns (c for a-l, and m, q for u-x).

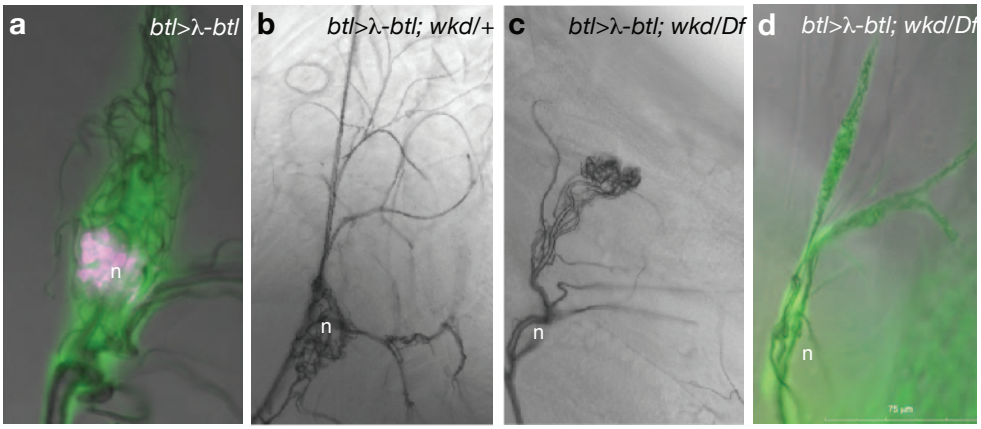

e

Genotype	*n*	Trachea			
		Distal OG* (%)	OG* Throughout (%)	Wildtype* (%)	Proximal* (%)
btl>λ-btl	37	0	3	14	84
btl>λ-btl; wkd$^{220/Df}$	39	31	38	18	13

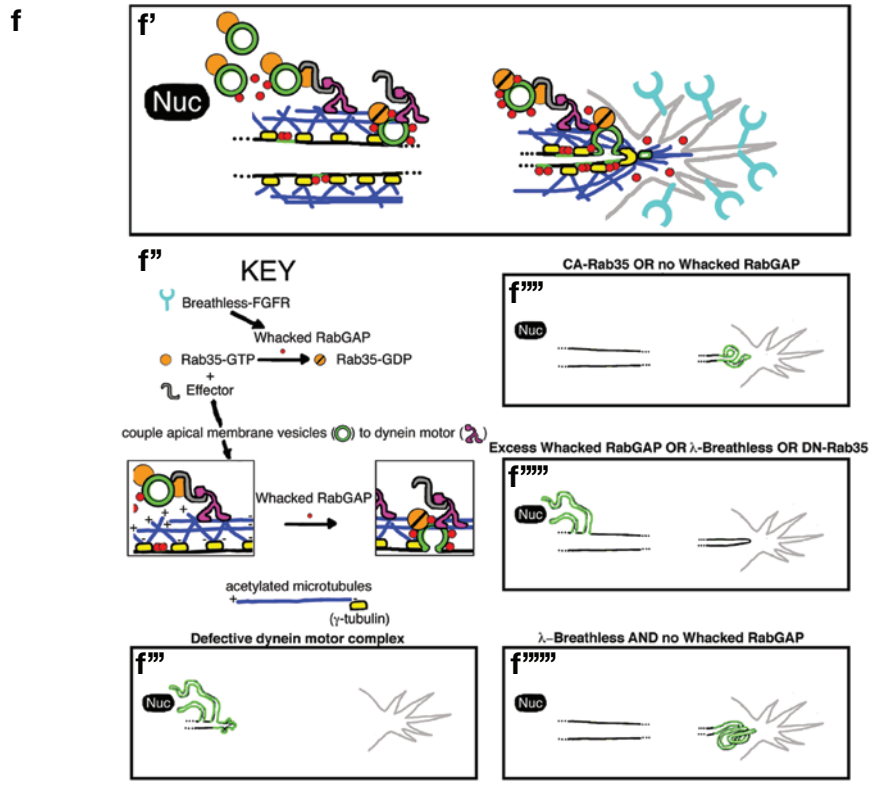

Figure S5 The Rab35/Whacked pathway regulates polarized growth of seamless tubes. (a) As shown in Figure 4k, activation of FGFR signaling in tracheal terminal cells results in the generation of ectopic tubes adjacent to the nucleus of the cell. In a *whacked* heterozygous background (b), the activated Breathless phenotype is unaltered. In a *whacked* mutant background (c, d), such ectopic tubes arise at more distal positions, sometimes exclusively at the branch tip, and sometimes more broadly distributed. In a *wkd* mutant background extra seamless tubes near the nucleus (n) are absent (c) or greatly reduced in number (d). (e) Table of data presented in a-d. (f) Model for Wkd/Rab35 polarization of seamless tube growth. In (f') we show an idealized terminal cell branch extending from near the terminal cell nucleus (Nuc) out to the growing tip of the terminal cell. The lumenal membrane is shown in black, with elipses (…) representing the space between the soma and branch tip. We hypothesize (see f'', KEY) that activation of Breathless, which triggers outgrowth of cytoplasmic extensions, also regulates Wkd so as to polarize seamless tube growth distally by catalyzing Rab35 GTP hydrolysis, resulting in liberation of vesicles from the transport apparatus. We propose that loss of dynein motor activity (f''') results in a failure to transport membrane components apically but also Rab35-vesicles distally, and so subsequently, these vesicles are added to the tube at nucleus proximal positions. In (f'''') the absence of Wkd Rab35GAP, or if Rab35 is constitutively active, seamless tube growth will be polarized at the cell tip. If Rab35 dominant negative is expressed, or excess Wkd Rab35GAP is expressed, or induced by constitutively active Breathless-FGFR (f''''), then transport of vesicles is blocked and addition to seamless tubes will occur proximal to the nucleus. Seamless tube will still be present distal to the soma since other vesicle transport pathways are able to promote tube growth in the absence of Rab35 activity. If Breathless-FGFR is constitutively activated but Whacked is absent from the cell (f'''''), then the ectopic seamless tube formation promoted by FGFR will be directed to the branch tips.

Movie S1 EB1:GFP dynamics in tracheal terminal cells. EB1:GFP comets can be seen moving in a bi-directional manner in regions adjacent to the terminal cell nucleus as well as more distal regions of terminal cell branches. Comets can also be seen extending from the apical membrane at a few branch positions more proximal to the cell nucleus. Near the soma, growth was towards branch tips at a 3:2 ratio (n= 50 comets scored), in medial positions growth was equally likely in either direction (~ 1:1, n = 41 comets scored), and near the end of the seamless tubes, there was a 2:1 distal bias (n = 28 comets scored). The first half of the movie extends over a 60 second interval and the second half of the movie extends over a 66 second interval and is being displayed at 10 frames per second.